

Improving estuary models by reducing uncertainties associated with river flows

Peter E. Robins^{a,*}, Matt J. Lewis^a, Jim Freer^{b,c}, David M. Cooper^d, Christopher J. Skinner^e, Tom J. Coulthard^e

^a Centre for Applied Marine Sciences, School of Ocean Sciences, Bangor University, Anglesey, UK

^b School of Geographical Sciences, University of Bristol, Bristol, UK

^c Cabot Institute, University of Bristol, Bristol, UK

^d Centre for Ecology and Hydrology, Bangor, UK

^e School of Environmental Sciences, University of Hull, Hull, UK

ARTICLE INFO

Article history:

Received 3 October 2017

Received in revised form

18 January 2018

Accepted 12 February 2018

Available online 2 March 2018

Keywords:

Estuary model uncertainty

River variability

Water quality

Climate change

Conwy

Humber

ABSTRACT

To mitigate against future changes to estuaries such as water quality, catchment and estuary models can be coupled to simulate the transport of harmful pathogenic viruses, pollutants and nutrients from their terrestrial sources, through the estuary and to the coast. To predict future changes to estuaries, daily mean river flow projections are typically used. We show that this approach cannot resolve higher frequency discharge events that have large impacts to estuarine dilution, contamination and recovery for two contrasting estuaries. We therefore characterise sub-daily scale flow variability and propagate this through an estuary model to provide robust estimates of impacts for the future.

River flow data (35-year records at 15-min sampling) were used to characterise variabilities in storm hydrograph shapes and simulate the estuarine response. In particular, we modelled a fast-responding catchment-estuary system (Conwy, UK), where the natural variability in hydrograph shapes generated large variability in estuarine circulation that was not captured when using daily-averaged river forcing. In the extreme, the freshwater plume from a 'flash' flood (lasting <12 h) was underestimated by up to 100% – and the response to nutrient loading was underestimated further still. A model of a slower-responding system (Humber, UK), where hydrographs typically last 2–4 days, showed less variability in estuarine circulation and good approximation with daily-averaged flow forcing. Our result has implications for entire system impact modelling; when we determine future changes to estuaries, some systems will need higher resolution future river flow estimates.

© 2018 The Authors. Published by Elsevier Ltd. This is an open access article under the CC BY license (<http://creativecommons.org/licenses/by/4.0/>).

1. Introduction

Understanding how estuaries may change in the future is of critical importance for mitigating against potential water quality degradation and flood risk changes. However, uncertainties in the current methodology are unclear and the accuracy of current techniques in determining changes to estuaries is unknown. Despite the clear importance of river-to-estuary transport in coastal water quality studies (e.g., Cloern, 2001; Lotze et al., 2006; Liu et al., 2014), biogeochemical, hydrological and hydrodynamic processes are often necessarily limited in both observations and in model

predictions; especially as one quantifies these fluxes at the national scale (Greene et al., 2015). Faced with a range of uncertainties in knowledge (e.g., instream biogeochemical processing (Monte et al., 2006; Malham et al., 2014)) and in model parameterisation and resolution (e.g., climate predictions of rainfall intensity (Charlton and Arnell, 2014), catchment predictions of runoff and ground-water flow (Fowler et al., 2007), or sediment transport parameterisation (Davies and Robins, 2017)), there is a real question as to whether model predictions of land-to-sea processes are useful in informing management decisions about water quality and ecological status (Jarvie et al., 2000). One important unknown is how sensitive estuarine models are to boundary forcing such as river flows, and what steps might be needed to improve their usefulness as a management tool for coastal water quality impact.

In the context of water quality management, within the

* Corresponding author.

E-mail address: p.robins@bangor.ac.uk (P.E. Robins).

European Union, the primary objectives of the Marine Strategy Framework Directive are to provide “good environmental status” and to “maintain biodiversity”, for all coastal waters by 2020. However, levels of nutrients and certain hazardous substances are overall still above acceptable limits and more efforts are needed to meet the 2020 objectives (COM, 2014). Globally, there is a growing concern that anthropogenic climate change is impacting the hydrological cycle, which may accentuate the degradation of coastal waters and ecosystems (Hannaford and Harvey, 2010; Robins et al., 2016). Nevertheless, it is unclear whether river flow dynamics have changed (e.g., Svensson et al., 2006; Hannaford and Marsh, 2008) or will change in the future (e.g., Kay et al., 2006; Wilby et al., 2008; Bell et al., 2012). Under the umbrella of the Marine Strategy Framework Directive, a suite of directives such as those for wastewater treatment and the control of nitrates, and other initiatives such as OSPAR (OSPAR, 2009) and (in the UK) the Marine and Coastal Access Act 2009, are being implemented to “future proof” against violations of Good Environmental Status and to reduce the vulnerability of coastal systems to climate change effects. Although issues translating from science to management have been apparent (e.g., Elliott et al., 1999).

One way that we can inform and improve coastal management strategies is to increase confidence in estuary modelling of fluxes and pollutant behaviour, by using climate model derived river flow projections downscaled to the most appropriate time step for the estuary (e.g., daily or sub-daily). This requires the next generation of climate models (GCMs and RCMs) that can improve their relevance to hydrological impact analyses (e.g., Cloke et al., 2013; Charlton and Arnell, 2014; Smith et al., 2014a, 2014b). Then, for example, we can explore the UK’s future projected “drier summers and wetter winters” signal and changes in storm types in more detail (e.g., Fowler et al., 2007b; Chan et al., 2013; Kendon et al., 2014). In this paper, therefore, we discuss the importance of resolving river flow temporal variability when understanding the dynamics of coastal systems and, ultimately, their management.

1.1. Processes affecting estuarine water quality

During low river flow conditions, the tidal pumping effect in estuaries generates a holding reservoir for substances upstream of the turbidity maxima (Robins et al., 2014). For instance, faecal indicator organisms that attach to suspended particulate matter (SPM) may be retained in the estuary and increase in concentration (Wilkinson et al., 2006; Malham et al., 2014). Large potential impacts in terms of water quality and public health risk then come when a high discharge event flushes the concentrated mass downstream into the estuary and coastal waters, possibly influencing shellfish beds and bathing waters (Naiman et al., 2008). Eutrophication from increased concentrations of nitrogen, phosphorus, and dissolved organic carbon in rivers has been shown to lead to toxic algal blooms in the estuary (Stratham, 2012; Tang et al., 2013; Liu et al., 2014). Storm events may also increase the delivery of untreated sewage to coastal waters, via combined sewer overflows or direct run-off (Rügner et al., 2014). Estuaries can become polluted from microbial contaminants, pathogens, and toxic substances like heavy metals, derived mostly from agricultural and industrial sources (e.g., consented discharges that are permitted by the Environment Agency in the UK), and can enter the food chain via uptake from benthic invertebrates (Arnell et al., 2015; Robins et al., 2016).

In the UK, the temperate maritime climate ensures relatively low flow variability on seasonal and inter-annual time scales, compared with catchments that experience snowmelt or monsoonal climates. However, because UK catchments are relatively small and often steep, flow variability at daily and sub-daily

time scales can be large and sensitive to the local rainfall intensity (Monk et al., 2006; Prudhomme and Davies, 2009a; 2009b) and local geology (catchment permeability), suggesting that management of such systems should be undertaken discretely (Wade et al., 2005). In addition, human influences such as flood control, irrigation, and power generation have the potential to alter natural flow patterns considerably, and especially at sub-daily timescales (Bevelhimer et al., 2015).

Yet, the sensitivity of these processes to high frequency river flow variability is poorly understood and poorly resolved in models (e.g., Wade et al., 2005). For many terrestrial substances, estuarine sensitivity to discharge-concentration dynamics (for which data is scarce) and how this varies for each storm, and over seasons and inter-annually, is also poorly understood. Therefore, reducing model uncertainties associated with the combined effects of river flow variability and discharge-concentration relationships is of importance for risk assessment and mitigation.

1.2. Estuary impact modelling and hypotheses

A suite of coupled simulations are needed to predict impact to estuaries over the coming century, which might necessitate bias correction changes in the climate model outputs, coupled with a wealth of input, boundary, parameter, and structure issues, together with the inherent uncertainties in the data (French and Clifford, 2000; Beven and Alcock, 2012; McMillan et al., 2012). In effect, an uncertainty ‘cascade’ is generated, with increased uncertainty further downstream as more models and data are linked (Lewis et al., 2011; Coulthard et al., 2012). For decision-making purposes, we need to quantify model uncertainties associated with present practices of estuarine and coastal impact studies, and determine whether GCMs/RCMs require downscaling to sub-daily rainfall and to be applied at higher spatial resolution in order to accurately simulate sub-daily river flows and estuarine impact (e.g., Coulthard and Skinner, 2016). Furthermore, will there be a clear difference in estuarine impact between slow-response systems (i.e., large or groundwater fed catchments) and fast-response systems (i.e., small or steep catchments without significant groundwater contributions)?

We study two contrasting catchment-estuary systems within the UK: a rapid-responding system, in which the transportation time through the river and estuary system is a few hours; and a slow-responding system, with comparatively long transportation times from river to sea. The two systems are described in Section 2. By characterising their river flow variabilities, we investigate the impacts upon estuarine and coastal circulation and mixing, with the aim of addressing the following hypotheses (in Section 3):

1. Rapid-responding systems are sensitive to sub-daily river flow variability; large epistemic uncertainties are simulated in estuarine fluxes, if models are driven by daily-averaged river forcing. Resolving the shape of the hydrograph in more detail will lead to more robust estimates of estuarine impact.
2. Slow-response systems are less sensitive to sub-daily river flow variability; modelled estuarine fluxes are well-represented by daily-averaged river forcing.

We are testing these hypotheses with two end members of estuary configuration (for the UK) to establish whether this is an issue for UK estuary modelling (and elsewhere in the world) and whether or not more studies would then be needed for the other estuaries. Finally, we discuss our results in Section 4, and the implications to future coastal impact modelling.

2. Case studies

2.1. Case study 1 (rapid-response system): Conwy, North Wales, UK (see Fig. 1)

The Conwy catchment and estuary represent a relatively small and pristine system on the west coast of the UK. The catchment area above the tidal limit is 380 km², draining much of the Snowdonia mountains. Annual rainfall varies between 500 mm near the estuary and 3500 mm in parts of Snowdonia. The geology is largely impermeable (Ordovician igneous and metamorphic rocks), and this, coupled with large elevation gradients, leads to rapid flow responses to rainfall; mainly <10 h for rainfall to reach the tidal limit (D. Cooper, *pers. comm.*). The River Conwy has a mean flow of 20 m³ s⁻¹, with Q95 and Q10 (i.e., 95th and 10th percentile flows) of 1.35 and 45.3 m³ s⁻¹, respectively, over the period 1965–2005. The catchment is mainly rural, with low to moderate intensity agriculture. Sediment and nutrient losses are small, although significant areas of upland peat lead to relatively high concentrations of organic carbon in some tributaries.

The Conwy estuary is characterised as an embayment type system that is macro-tidal (i.e., 4–6 m tidal range), where, under mean conditions, the tidal volume exchange dominates over the river input (Davidson et al., 1991). The estuary is relatively small, extending 20 km in length. Strong tidal mixing results in a vertically near-homogeneous salinity structure for the majority of the tidal cycle (Simpson et al., 2001; Howlett et al., 2015). Robins et al. (2014) showed that mixing length scales were controlled to a greater extent by river flow magnitude, than the tidal excursion. This result implies that, for this system, the transport of river-borne material (dissolved and particulate) through the estuary is largely determined by the river flow, with lesser modification due to the tide. However, Robins et al. (2014) used constant flowrates in their simulations and they did not investigate the sensitivity of the system to sub-daily river flow variability. We retain bathymetric data for model development, and extensive observational data enabling model validation and input parameterisation (see Appendix).

2.2. Case study 2 (slow-response system): Humber, East England, UK (see Fig. 1)

The Humber catchment covers 24,000 km² and contains one of the largest river networks in the UK, made up of two main tributaries, the Ouse (via the Derwent, Swale, Ure, Nidd, Wharfe and Aire) and the Trent (via the Derwent and Dove) (Law et al., 1997). The distance from headwaters to coast is approximately six times longer than for the Conwy, with shallower gradients. The basin geology is permeable, being formed of carboniferous millstone grits and limestones in the uplands, and the lower reaches run over glacial and fluviually worked sands and gravels (Law et al., 1997). Rainfall varies from 1600 mm per annum in the upland regions to 600 mm near the estuary (Law et al., 1997). Combined, the average fluvial input to the estuary is 250 m³ s⁻¹ (high flow = 1600 m³ s⁻¹), with Q95 and Q10 (percentile flows) of 58 and 610 m³ s⁻¹, respectively, over the period 1980–2015; yet, despite these significant fluvial inputs, the estuary is characterised as tidally dominant and well-mixed (Townend and Whitehead, 2003).

The Humber estuary is characterised as a large coastal plain system (Davidson et al., 1991), which extends 120 km, with the mean spring tide having a range of 5.7 m, i.e., macro-tidal (Mitchell et al., 1998). During winter periods, where fluvial flows into the estuary are higher, the freshwater-saltwater interface and the estuarine turbidity maximum are located near Hull (30 km inshore from the estuary mouth). During the lower flow periods in the

summer, they have been observed up to 95 km inland (Uncles et al., 1999, 2006). A sediment budget for the Humber estimated by Townend and Whitehead (2003) showed that, during mean tidal conditions, fluvial sources contributed 335 tonnes per tide of sediment to the estuary, which was 0.3% of the marine contribution. For the purpose of developing the estuary model, we have access to extensive bathymetric, flow and stage (water level) data for the Humber estuary.

3. Methods and results

To address our hypotheses, we quantify the realistic variance in observed river hydrograph shapes at sub-daily resolution for our case study catchments. Developing hydrodynamic models, first of the Conwy and then the Humber, we simulate a range of representative hydrograph shapes, under different tidal conditions, to determine the level of misrepresentation of estuarine circulation, caused by using lower resolution daily-mean river flow forcings.

3.1. Fast-responding systems

For the river Conwy, flow data from a gauging station near the head of the Conwy estuary was attained from Natural Resources Wales. The location was Cwm Llanerch (gauging site reference 66011; labelled 'Conwy' in Fig. 1b), which is just beyond the tidal influence in the river. Time series were available from 1980 to 2015, inclusive, at 15-min intervals, thereby enabling flood hydrographs during this period to be isolated and their shape analysed. The data set was 99% complete. Considering the 36-year series, 1689 separate discharge 'events' were isolated for our subsequent analysis, based on our criteria of having a volume discharge larger than the mean volume discharge of all discharge events during the series, where a discharge event was defined as having a peak flow greater than the mean flow (e.g., Fig. 2a). This criteria was chosen so that the most prominent storms were selected. The selected discharge events ranged in peak magnitude from 27 m³ s⁻¹ to 550 m³ s⁻¹ (mean = 179 m³ s⁻¹, standard deviation = 99 m³ s⁻¹), and each event generally lasted between 12 and 24 h.

So that we could examine each of the 1689 hydrograph shapes, relative to one another, the events were fitted, after scaling, to the curve of a two-parameter gamma probability density function, defined by:

$$f(x; k, \theta) = \frac{x^{k-1} e^{-x/\theta}}{\theta^k \Gamma(k)} \quad [\text{for } x > 0 \text{ and } k, \theta > 0] \quad (1)$$

where x is time, k and θ describe the shape and scale of the curve, respectively, and $\Gamma(k)$ is the gamma function evaluated at k . Since hydrographs are characteristically skewed, the gamma function has been found to give a good approximation to the measured rainfall response of rivers (see Haktanir and Sezen (1990) and Jayawardena (2014) for more details on gamma distributions). Events that were very close to one another (e.g., peak flows < 6 h apart) were not analysed. Prior to fitting the curve, each hydrograph was shifted to originate at [0, 0] and scaled down so that the integral of the hydrograph equalled one, which defines a gamma probability density function. We scaled in both time and magnitude so that the original hydrograph shape was unaltered (for subsequent simulations, each gamma curve was scaled back up to the original size to represent the measured hydrograph).

As examples, Fig. 2b and c show the gamma curve fitting procedure for selected hydrographs during the summer of 2012, and the following winter, respectively; notice that the two gamma curves have different shapes, when fitted to the scaled hydrographs. The

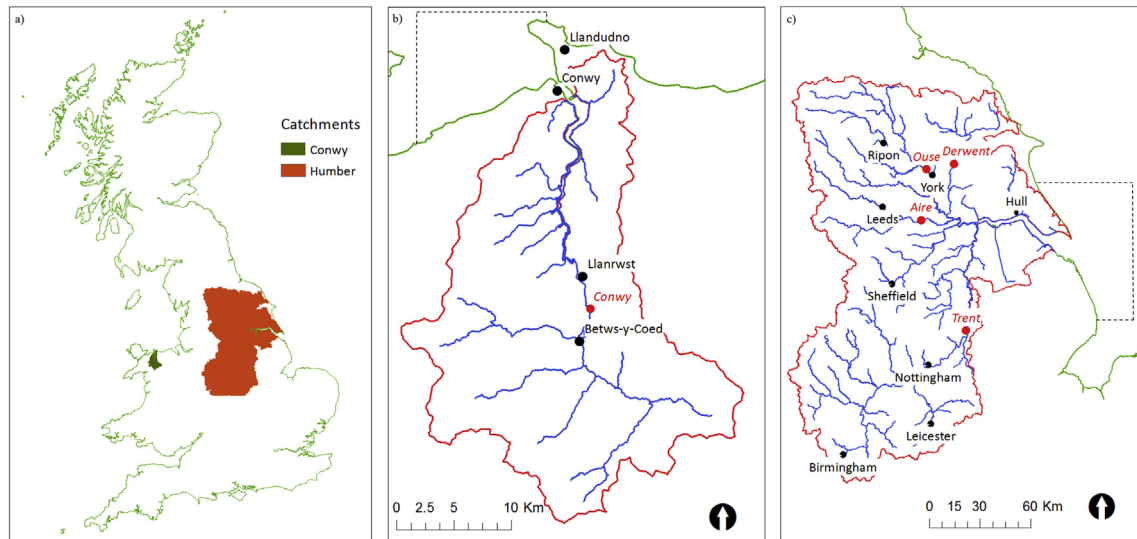


Fig. 1. a) Map of the UK, showing the two case study regions, the Conwy catchment and estuary and also the Humber catchment and estuary. Detailed maps of the (b) Conwy catchment and estuary and (c) the Humber catchment and estuary are shown. In each case, the estuary and model boundary is shown (dashed line). Key urban areas are labelled (black) and also the river gauging stations analysed in this study (red). (For interpretation of the references to colour in this figure legend, the reader is referred to the web version of this article.)

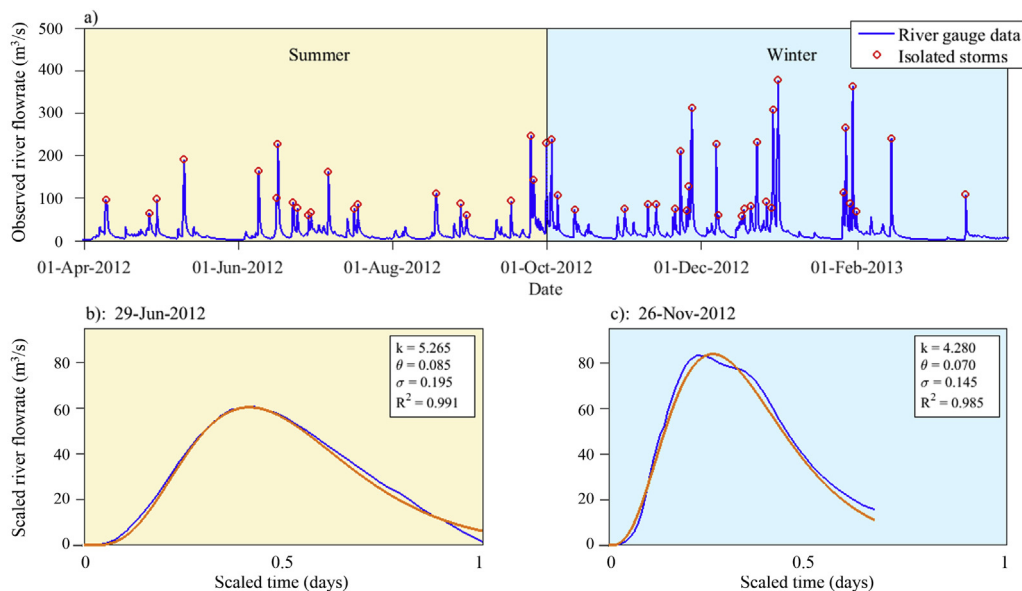


Fig. 2. a) Sample section (01 April 2012 – 31 March 2013) of the Cwm Llanerch river gauge time series, showing the storm events that we isolated for analyses. The entire 36-year time series analysed was from 1980 to 2015, at 15-minute resolution. As an example, (b) and (c) show representative storm hydrographs during ‘summer 2012’ and ‘winter 2012/13’, respectively (blue curves). A two-parameter gamma distribution curve was fitted to each hydrograph (e.g., orange curves), so that their shape (k) and scale (θ) can be approximately quantified. R^2 values refer to the goodness of fit for each fitted (Pearson’s correlation). The curves have been scaled in magnitude and time for comparison of their shape. (For interpretation of the references to colour in this figure legend, the reader is referred to the web version of this article.)

winter curve shows a more rapid response, and is described as more ‘flashy’ than the summer curve. For our subsequent analysis, the standard deviation, σ , of each fitted gamma curve were calculated, defined as $\sigma = \sqrt{k\theta^2}$. We use σ as a measure of the flashiness of each hydrograph; the smallest values of σ indicating most flashy and largest values indicating least flashy (e.g., Fig. 3a).

In order to simulate the range of realistic discharge events entering the Conwy estuary, an ocean model (TELEMAC-2D [V7.0]; www.opentelemac.org) was applied to the case study region. Model details and a description of its parameterisation and assumptions are presented in the Appendix. We initially simulated a

representative ‘flash flood’ river scenario, where we compared a simulation with 15-min flow forcing to a simulation with daily-averaged flow forcing (RUN-1a; see Fig. 3b and Table 1). Similarly, we then simulated a representative ‘slow flood’ river scenario, where again we compared 15-min and daily-averaged flow forcing (RUN-2a; see Fig. 3c and Table 1). Our simulated flash and slow hydrograph shapes represent the realistic range of discharge events for the 36-year series. Specifically, from the whole sample of gamma fitted functions, we take the function with σ closest to the 5th percentile to represent the flash flood. Likewise, we take the function with σ closest to the 95th percentile to represent the slow

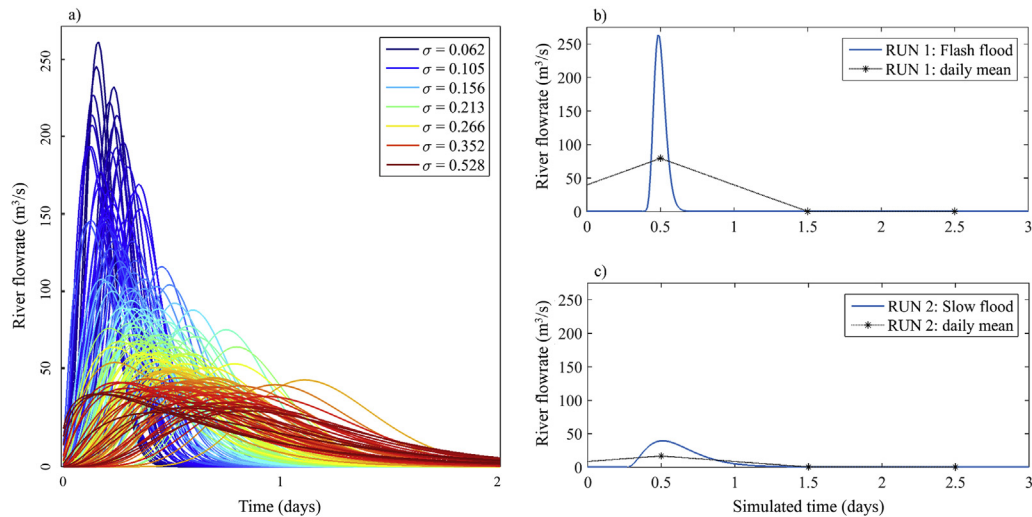


Fig. 3. Panel (a) shows selected two-parameter gamma curves that were fitted to the storm event hydrographs to characterise their shape. The gamma curves from 1,689 separate flood hydrographs were sorted with respect to their standard deviation, σ (lowest-to-highest), and every 10th curve has been plotted (i.e., totalling 168 curves). The legend displays the standard deviation value for every 25th curve plotted, showing increasing standard deviation (blue through to red curves) represents a decrease in hydrograph ‘flashiness’. These curves and the pattern described are representative of the entire series. Panel (b) shows the hydrograph that was used for the estuarine simulation that represents a realistic flash flood event; i.e., a ‘flashy’ gamma curve was selected from the analysis and scaled-up to represent the corresponding river flow magnitude and duration. Similarly, panel (c) shows the hydrograph that was used for the slow flood event. In both scenarios, the simulations were compared to the daily-mean river forcing. (For interpretation of the references to colour in this figure legend, the reader is referred to the web version of this article.)

Table 1

TELEMAC-2D simulations. RUN-1 and RUN-2 were simulations with the Conwy estuary model, whereas RUN-3 and RUN-4 were with the Humber estuary model. N denotes the number of discharge events analysed to produce the representative ‘flash’ and ‘slow’ hydrographs, where k and θ describe their shape and scale, respectively, and σ represents their standard deviation. For each scenario, a comparative simulation with daily-averaged river forcing were also produced.

Simulation	Tide at mouth relative to peak river flow at tidal limit	River forcing hydrograph shape				
		N	k	θ	σ	
RUN 1 (Conwy flash flood)	a) Flood tide	Conwy:	1689	10.5	0.02	0.08
	b) Slack water					
RUN 2 (Conwy slow flood)	a) Flood tide	Conwy:	1689	7.63	0.09	0.26
RUN 3 (Humber flash flood)	a) Flood tide	Aire:	868	4.68	0.08	0.18
		Derwent:	678	4.57	0.23	0.49
		Ouse:	637	4.45	0.10	0.20
		Trent:	599	6.10	0.10	0.24
RUN 4 (Humber slow flood)	a) Flood tide	Aire:	868	2.82	0.27	0.46
		Derwent:	678	1.81	0.91	1.22
		Ouse:	637	3.44	0.24	0.44
		Trent:	599	3.51	0.30	0.56

flood. In each case, we scale-up the function to closely match the actual corresponding flows; so in this circumstance, the flash flood had a peak flowrate of $260 \text{ m}^3 \text{ s}^{-1}$, and the slow flood was much smaller, with a peak flowrate of $\sim 50 \text{ m}^3 \text{ s}^{-1}$, as shown in Fig. 3b and c, respectively.

Each simulation was spun-up from initial conditions to steady-state conditions (see Appendix), and then run for a further 15 days, with peak flows occurring after 12 h, and baseflow conditions ($0.3 \text{ m}^3 \text{ s}^{-1}$) resuming after the event had passed. For the daily-averaged flow simulations, flow values were assigned at midday and the model then linearly interpolated to the model time step (see Fig. 3b and c, which show the initial 3 days of river forcing). Tidal forcing comprised the principal lunar semi-diurnal tidal constituent, M_2 (period of 12.42 h), with an amplitude 2.6 m, representing mean tidal conditions for the Conwy (see ntslf.org). Peak river flow at the tidal limit coincided with peak flood tide at the estuary mouth. Note that we do not simulate tidal range variations, such as spring-neap cycles. Whilst this can be computed relatively easily, we have simplified the tidal forcing so that we can concentrate on river flow simulated variabilities.

3.2. Estuarine saline response to river forcing

Firstly, we compare the saline response in the estuary to the flash flood event (RUN-1), forced with both 15-min and daily-averaged flows (see Fig. 3b). The two simulations show a markedly different spatial extent to the freshwater plume, because the daily-averaged approximation did not capture the peak magnitude of the freshwater event (Fig. 4a and b). The time-dependent total salt in the estuary was calculated for RUN-1 and RUN-2. We show a reduction in total salt, due to the passing of the high discharge event, and we show the saline recovery afterwards via the tidal pumping mechanism (Fig. 4c and d). For the flash flood event (RUN-1), our main and most striking result is that, when daily-averaged flows were applied, the total amount of salt in the estuary ($\sim 4 \times 10^8 \text{ kg}$) was more than double that simulated with 15-min river flows (Fig. 4c). This impact is a significant misrepresentation in the widespread dilution factors over a considerable period – saline recovery to within 75% of the pre-event levels took approximately 3 days, and 1 week for 95% recovery; this pattern was not captured with the daily-averaged flow simulation. This

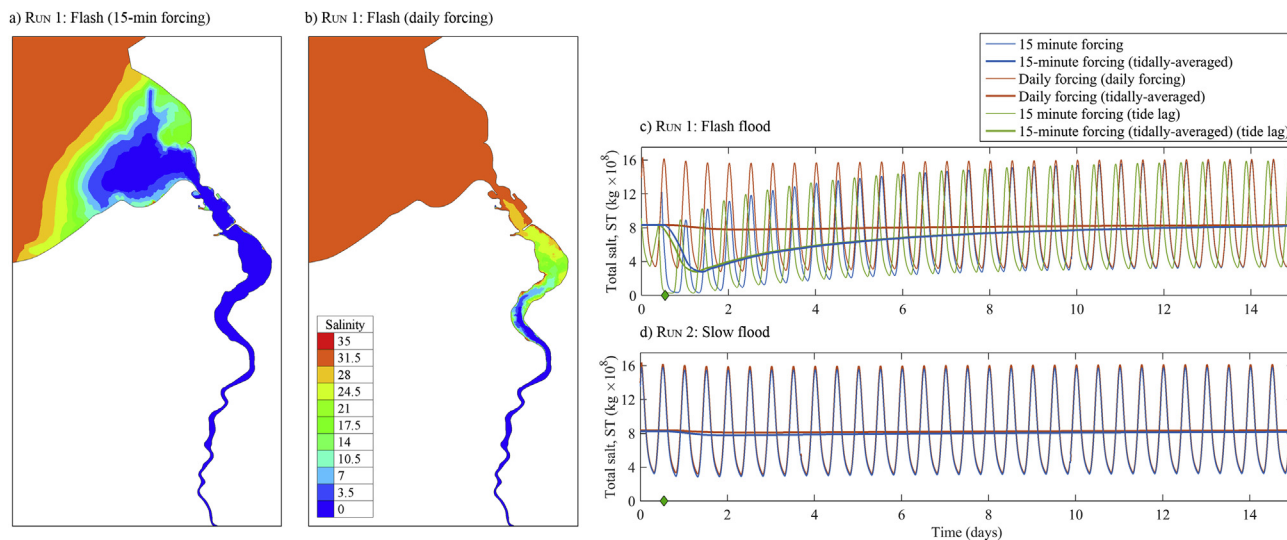


Fig. 4. Conwy estuary simulations of salinity. For the flash flood event simulations (RUN-1, see Fig. 3b), we show spatial differences of the maximum freshwater plume, between (a) 15-minute river forcing and (b) daily river forcing. In panels (c) and (d), we show total simulated salt content in the estuary over 15 days, and the timing of peak flowrates is denoted by the green diamond. For the flash flood event simulations (panel c), we highlight up to 50% difference between the modelled output forced with 15-minute river data (blue curves) and daily-averaged data (red curves). The green curves represent 15-minute river forcing with a tidal phase lag. For the slow flood event simulations (panel d), we show less (~3%) difference between the modelled output forced with 15-minute river data (blue curves) and daily-averaged data (red curves). (For interpretation of the references to colour in this figure legend, the reader is referred to the web version of this article.)

important result suggests that, for the Conwy system, it is misleading to use daily-averaged river flows to infer the estuarine response. The simulation was for a particularly flashy and high peak magnitude event (i.e., $\sim 260 \text{ m}^3 \text{ s}^{-1}$), suggesting that the ‘factor of 2’ discrepancy represents near maximal model uncertainty for this system.

To demonstrate that the timing of the discharge event, relative to the tidal exchange, is less important than the hydrograph shape, we repeated the flash flood simulation, but with peak flowrates occurring during at slack water, rather than during peak flow (RUN 1b; see Table 1). We simulated very little difference in the total estuarine salt content (other than the expected 3-h shift in the response), and similar saline recovery rates, between RUN-1a and RUN-1b (Fig. 4c).

The slow flood event (RUN-2) reduced the steady-state estuarine salt content only slightly, and the daily-averaged approximation was similar (within 5%) to the simulation with 15-min flows (Fig. 4d). This was because the daily-averaged approximation was much closer to the 15-min hydrograph, and because the simulation depicted a particularly low peak magnitude event (i.e., $\sim 50 \text{ m}^3 \text{ s}^{-1}$). In both scenarios, the recovery timescales were approximately 2 weeks (i.e., the maximum amount of salt was within 10% of the initial maximum level, given a post-event constant flowrate of $0.3 \text{ m}^3 \text{ s}^{-1}$, which represents minimum flow conditions).

3.3. Estuarine retention of nutrients

Our simulations have implications for the estuarine retention of river-borne material, such as dissolved and particulate macronutrients and pathogenic viruses. A recent and intensive macronutrient survey conducted in the Conwy catchment has revealed that the relationship between particulate nutrient concentrations (mg L^{-1}) and flow Q ($\text{m}^3 \text{ s}^{-1}$) can be approximated by $C_n = F_n(1 + 0.025Q)^2$, where the multiplier F_n equals 0.07 for particulate organic carbon (C_{POC}) (Fig. 5a). Particulates were found by differences between total and dissolved components. Standard errors for the parameters are approximately one tenth of the values themselves, with R^2 values of the order 0.7. C_{POC} can also be used as a

proxy for viruses, as they adhere to particles or are contained in bacteria so would appear in the POC/floc fraction (D. Jones, *pers. comm.*).

We inputted nutrient concentrations equivalent to C_{POC} at the river boundary for RUN-1 and RUN-2, and the total estuarine nutrient content was calculated in a similar way to the salt content. At the start of the simulations, the estuarine C_{POC} content was zero. For the flash flood event, the simulated total estuarine C_{POC} concentrations are plotted in Fig. 5b, showing a considerable underestimation in particulate carbon concentration when forced with daily-averaged flows. In our case, peak amounts of particulate carbon were expected to be $14 \times 10^3 \text{ kg}$, based on 15-min river flows, but only $1 \times 10^3 \text{ kg}$ were simulated with daily-averaged river flows (Fig. 5b). C_{POC} concentrations were still under-predicted by RUN-2, by a factor of three, one week after the flood event, and concentrations returned to background levels after approximately two weeks, which represents for this case the prolonged period of large uncertainty when using daily-averaged forcing. We recognise that there are other processes that might change the C_{POC} signal over time that are not being treated here and would be the case also for other nutrient and pathogen behaviour to varying degrees.

3.4. Slow-responding systems

To address hypothesis 2, we chose the Humber estuary as a contrasting system to the Conwy, being a slower responding catchment (rainfall taking approximately twice as long to reach the estuary) and much larger estuary, but with a similar tidal range. Our model comprised bathymetry data (at 100 m spatial resolution) from an existing validated Humber estuary model (see Skinner et al., 2015). Tidal forcing was driven by a sinusoidal water-level of 2.34 m amplitude and 12.42 h period, which corresponds to the mean tidal conditions at the Humber (see ntslf.org).

We analysed high discharge events for the four primary rivers entering the Humber estuary; namely, the River Aire (Station 27003), River Derwent (Station 27041), River Ouse (Station 27009), and River Trent (Station 28022) (Fig. 1c). River gauge data were provided by the Environment Agency. The hydrograph peaks from

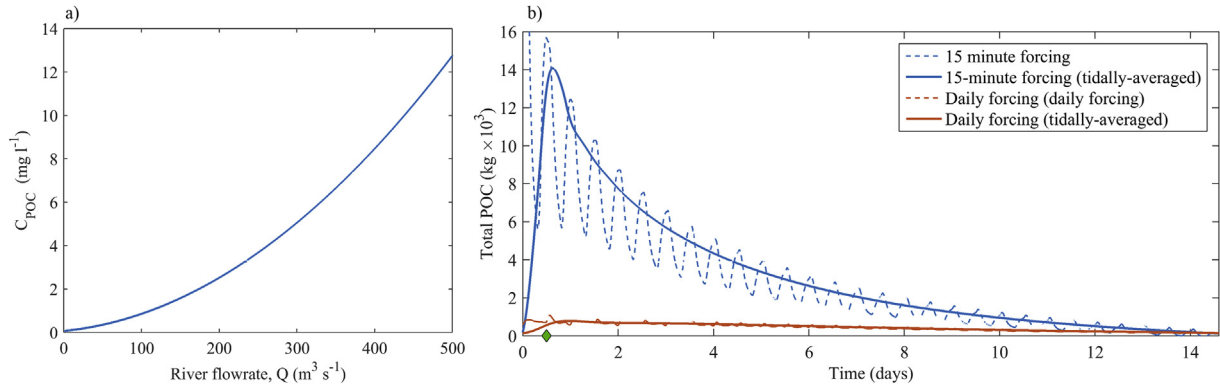


Fig. 5. Panel (a) shows the relationship between river flowrate and particulate organic carbon (C_{POC}), based on measurements from the Conwy estuary, where $C_{POC} = 0.07(1 + 0.025Q)^2$ and Q is the river flowrate at the river boundary of the model. In panel (b), we show total simulated POC content in the estuary over 15 days, from the flash flood event simulations. The timing of peak flowrates is denoted by the green diamond. We show a large (>90%) miss-representation of POC when forced with daily-average river forcing (red curves), compared with 15-minute river forcing (blue curves). (For interpretation of the references to colour in this figure legend, the reader is referred to the web version of this article.)

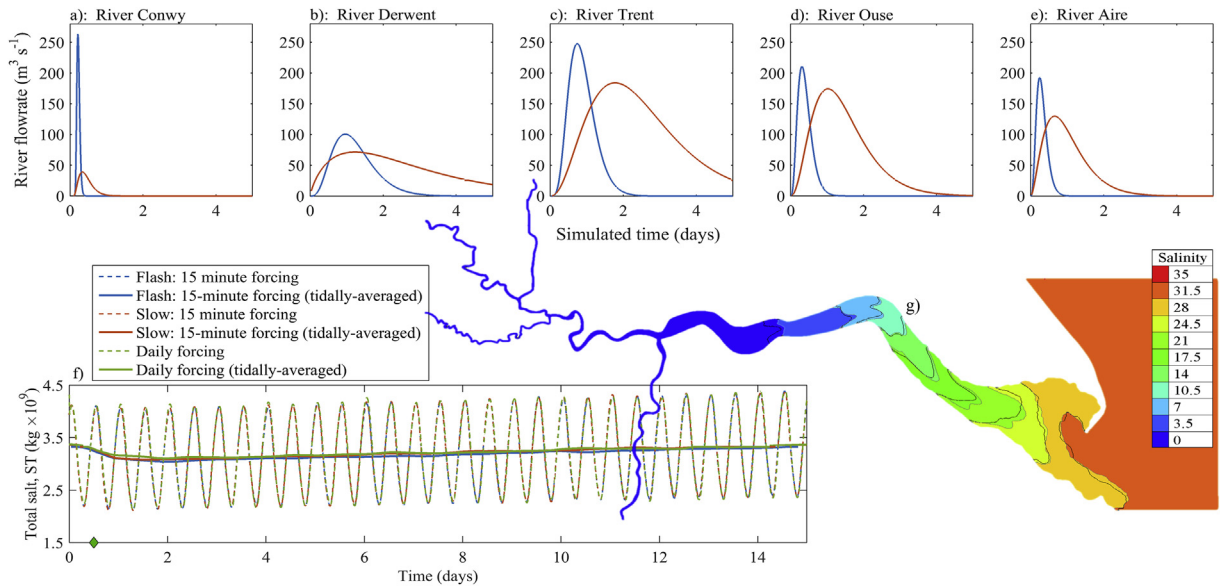


Fig. 6. Humber estuary simulations of salinity. Panels (a–e) show river forcing applied in the models (blue curves: flash flood, red curves: slow floods). Panel (a), for the Conwy, is shown only for comparison with the Humber rivers (b–e). The hydrographs represent curve fitting to the river gauge data. Panel (f) shows the Humber estuary simulated response to both flash (blue curves) and slow (red curves) events, in terms of total salt content during the 15-day simulations. Additionally, the estuarine response to the flash flood event with daily-averaged river forcing is shown (green curves). The timing of peak flowrates is denoted by the green diamond. For the flash flood event, the spatial differences of the maximum freshwater plume, between 15-minute river forcing (coloured contours) and daily river forcing (shifted black contour lines) is shown in (g). (For interpretation of the references to colour in this figure legend, the reader is referred to the web version of this article.)

all four tributaries generally occurred at the river gauges at similar times, and also travelled into the estuary over similar timescales. Mirroring the above methodology, each river gauge sampled at 15-min intervals and the analysed period was from 1980 to 2015. In comparison to the River Conwy (Fig. 6a), the range of hydrograph shapes for the rivers entering the Humber were markedly ‘slower’, as demonstrated in Fig. 6b–e and quantified by generally higher values of σ in Table 1. In addition, variability in hydrograph shapes were slightly greater in the Humber (i.e., $\Delta\sigma$ was 0.18 in the Conwy and 0.24–0.73 in the Humber, where we define $\Delta\sigma$ as the difference between the flash and slow σ values; see Table 1).

Two final scenarios were simulated with the Humber estuary model (see Table 1). RUN-3 represents a flash flood scenario, where each of the four river boundaries were forced simultaneously with the flash flood hydrographs calculated by our curve-fitting analysis, followed by baseflow conditions (0.85, 4.5, 2.5, and 1.75 $m^3 s^{-1}$), as

displayed in Fig. 6b–e, respectively. Similarly, RUN-4 represents a slow flood scenario, as depicted by the slow flood hydrographs in Fig. 6b–e. As shown in the figure panels, each hydrograph was scaled to represent the corresponding magnitude and duration of the flow data. As for the Conwy, the two Humber simulations were repeated with daily-averaged river forcing, rather than 15-min forcing.

Our simulations indicate that the Humber showed low sensitivity to the natural range of river flow hydrographs; the total amount of salt retained in the Humber estuary varied by <3% between the flash flood (RUN-3) and slow flood (RUN-4) scenarios, even though the combined freshwater volume discharge for the slow scenario was larger (Fig. 6f). This is because the estuarine volume is sufficiently large that the fluvial input has a less pronounced influence, compared with smaller estuaries like the Conwy. We re-simulated the events, but forced with daily-averaged

flows, and the estuarine response did not markedly change; the flash flood event simulation over-estimated salt content by <4% (Fig. 6f and g). This is because, unlike the flood events in the Conwy (that lasted <24 h), the Humber hydrographs were much slower (events lasted 1–5 days) and better approximated by daily-averaged flows. This result implies that, for the Humber system, daily-averaged river flows provide a good representation of the estuarine response.

4. Discussion

4.1. Estuarine impact modelling

Using two contrasting examples, we highlight the sensitivity of a small and impermeable catchment-estuary to high frequency river flow variability; the sensitivity being caused primarily by the relative influence of the river volume to the estuary volume. This result implies that other sensitive and quick responding systems may need careful application of river boundary forcing in order to simulate a meaningful response. Daily-averaged river forcing, commonly output from catchment models, may mask much higher magnitude flash flood events that last only a few hours and affect the estuary dynamics and loading in a markedly different way. However, quantifying and translating the importance of model uncertainties to issues such as water quality degradation, coastal flooding, erosion, fisheries, or to other forms of impact is case-specific. From this study, we anticipate daily-forced model uncertainty to be greatest for smaller systems that experience high-magnitude flash flood events due to, for example, steep or impermeable catchments. We compared the estuarine response of particularly flashy and high-magnitude river events with the daily-averaged approximation – the difference in estuarine response broadly representing the maximum modelled uncertainty caused by daily-averaged forcing.

Our sample size (of two estuaries) is too small to extrapolate our results to all estuaries. We have deliberately chosen estuaries at the two ends of UK estuary size and morphological typology, to investigate the issue of river flow variability. Therefore, these two systems cannot be representative of all UK estuarine systems, but provide us with examples of how river flow variability *can* be a major issue influencing model outcomes and forecasts. These findings should therefore be taken into account when designing or setting up model runs for estuary systems in the UK and worldwide.

Nevertheless, our results lead us to suggest that when the size of the storm hydrograph relative to the estuary (e.g., a fraction defined by the hydrograph volume divided by estuarine volume; Savenjie, 2006) is large, then the hydrograph shape should be resolved for impact studies (i.e., the sampling frequency is at least twice the representative frequency; Landau, 1967). For the Conwy flash flood scenario (Run 1), we estimate the river influence fraction to be 4% (i.e., the hydrograph volume was 367,490 m³ and the estuary volume at mean sea level was 8,943,740 m³). For the Humber flash flood scenario (Run 3), the river influence fraction was 1.45% (i.e., the combined hydrograph volume was 41,865,984 m³ and the estuary volume was 2,890,192,750 m³).

Determining the particular threshold of relative storm hydrograph size for impact will depend to some extent on application (e.g., to flooding or water quality), and will require more estuary types to be simulated. Nevertheless, we have attempted to estimate thresholds for the Conwy and the Humber by simulating some additional scenarios (see Fig. 7). We varied the river storm volume (keeping the hydrograph shapes unchanged, see Table 1) and calculated the resultant reduction in total estuarine salt. By assuming that impact was represented by a 10% salt reduction

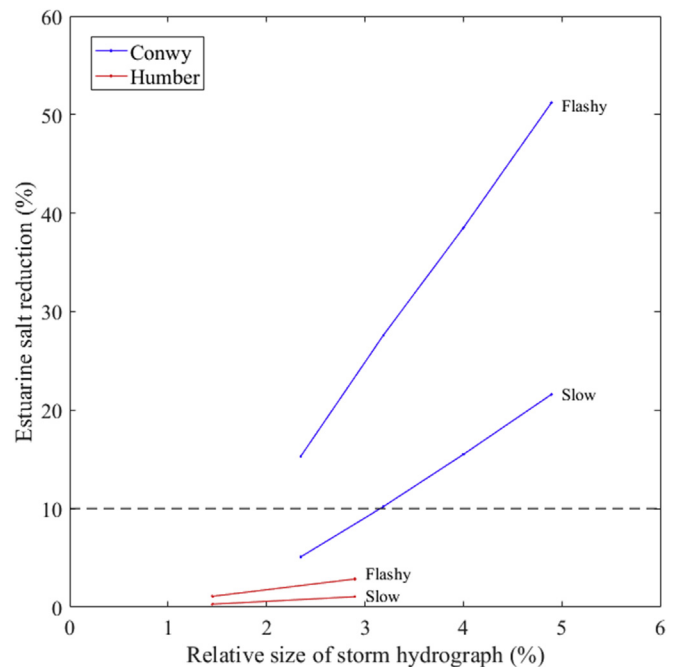


Fig. 7. Size of storm hydrographs in relation to estuary volume (%) plotted against estuarine impact in terms of total salt reduction (%), for different hydrograph shapes simulated in the Conwy and Humber. River volumes were calculated over the period of the storm hydrograph. Estuary volumes were calculated at mean sea level. Salt reduction was calculated relative to low-flow conditions, over a period of one week.

depicted, as shown in Fig. 7, the significance of different sized and shaped hydrographs becomes clear. For the Conwy, flashy hydrographs greater than ~2% of the estuary volume reduce the salt content by > 10% (as we've seen from our previous simulations, capturing this impact requires the hydrograph to be resolved). Whereas slow hydrographs require greater river volumes (e.g. exceeding 3% of the estuary volume) to achieve similar impact. However, a general result for the Conwy and Humber is not evident from Fig. 7, suggesting that additional and contrasting systems should be studied in future work.

For application to future impact studies, an important question then arises: Is projected 'change' of magnitude of river events and expected loads in the future more important than present-day variability in storm 'type'? Here, we only investigate 'type' and suggest that natural variability is important for estuaries that show sensitivity. It is not clear whether the uncertainty quantified here is more significant than other uncertainties in climate models (e.g., emission scenarios, downscaling from global to regional scales, parameterisations such as land cover, or predictions of rainfall). If we assume that storm type is not likely to change in the future, then our methods for characterising river flow variability can be applied for future impact studies. If, however, precipitation patterns are to change so that estuarine circulation is affected beyond natural variability (e.g. Fowler et al., 2007b; Christerson et al., 2012; Kay and Jones, 2012; Prudhomme et al., 2012; Charlton and Arnell, 2014), or if land use changes in a way that affects river flow variability, then these additional impacts need to be resolved and for certain estuaries will require sub-daily quantification of type changes to ensure meaningful predictions can be made. Systems near a tipping-point for impact (e.g., the Conwy in Fig. 7) may therefore be more sensitive to changes in the climate than systems away from such a tipping-point (e.g., the Humber in Fig. 7).

Hence, our results could stimulate a wider and more detailed analysis. For example, future work could address the following key

questions: (1) Will storm hydrograph shapes change in the future?; (2) What is the influence of storm clustering?; (3) What temporal resolution river flows are needed and how important is this in relation to other model uncertainties; and (4) How should climate and catchment models be parameterised and downscaled to be able to simulate river flows at the most appropriate temporal resolution? On the other hand, we could ask how important the role of all the smaller estuaries is compared to that of the fewer larger ones in the UK? There is a tendency to focus on the largest rivers – whereas the contribution of the many smaller ones is unclear. Also, how important is estuary type/shape compared with the river flow variability? To our knowledge, such comparative studies have not been conducted. We have shown results between estuaries may not be easily transferrable, this suggests we require national modelling frameworks to be developed that include relevant coupled hydrodynamics of estuarine processes for effective future impact characterisation.

We looked for climate trends in the hydrograph shapes analysed here (Conwy, Aire, Derwent, Ouse, and Trent), seasonally and inter-seasonally. We found that the mean hydrograph shape during winter (October–March) was generally flashier than during summer (April–September) (results not shown), since the catchments are generally more saturated during winter (because rainfall is generally higher and evaporation lower although high discharge events occur throughout the year in the UK, and there is much spatial variability). We also looked at the mean shape of the five most flashy hydrographs per season, to see if a catchment has become more or less flashy over time, although there were no significant trends over the natural variability (results not shown).

The North Atlantic Oscillation (NAO) index can be used as a measure of the inter-annual variability of storminess patterns across Europe (Hurrell, 1995; UKCP09). A positive NAO index tends to lead to increased westerlies and mild and wet winters. In contrast, for negative NAO index months, northern Europe experiences cold and dry winters with northerly storms (UKCP09). For

the Conwy, there appears to be a significant linear correlation between hydrograph shape and variations in the December–January–February NAO index (Fig. 8). The correlation indicates that positive NAO winters will produce more flashy hydrographs, while negative NAO winters will produce less flashy hydrographs. When applied to the Humber rivers, however, there were no significant correlations between hydrograph shape and NAO (results not shown). This may be because of the longer response times in the Humber catchment, or that the weather patterns in the eastern UK are significantly different, compared with the western UK (predominant westerlies will favour high flows in the western UK). However, correlations between the NAO and river flow variability have previously been found (e.g., Trigo et al., 2004). Yet, the causes of past and probable future NAO variations are still unclear; further, no current RCMs can accurately predict these trends or project future trends with any certainty (UKCP09).

5. Conclusions

Estuarine circulation represents a crucial pathway in the hydrological cycle, where both terrestrial and ocean processes interact within a confined and changeable environment. We highlight the sensitivity of small systems to sub-daily variations in storm discharge and associated nutrient loads. This has implications for future estuary/coastal impact studies, where downscaling daily river flow projections from climate models is poorly understood.

A curve-fitting analysis was applied to river gauge data (1980–2015) in order to identify representative storm hydrograph shapes for a small estuary that responds quickly to rainfall (<1 day). Using these representative storms as river forcing, we simulated estuarine dispersal of salinity and nutrient concentrations. Large differences were produced when forced with daily-averaged flows, compared with simulations with 15-min flows. Further, the influence of large storms on estuarine water quality tended to last up to two weeks, which was not captured when forced with daily-averaged flows.

In contrast, when the above method was applied to a slower-responding catchment (i.e., storm hydrographs typically lasting 2–4 days) connected to a larger estuary basin, the uncertainties from daily-averaged approximations were negligible. Which systems require downscaled modelling methods and which do not, therefore requires further investigation, and is likely influenced by the combined size and shape of the catchment shape and estuary, together with anthropogenic factors and climate trends.

Acknowledgements

P. Robins and D. Cooper wish to acknowledge the NERC-funded Macronutrients Cycles Programme (Turf2surf project: NE/J011967/1) and the NERC-funded Environmental Microbiology & Human Health Programme (Viraqua project: NE/M010996/1). P. Robins and M. Lewis wish to acknowledge the support of the Sêr Cymru National Research Network for Low Carbon, Energy and the Environment (NRN-LCEE) project QUOTIENT, the SEACAMS research project (Sustainable Expansion of the Applied Coastal and Marine Sectors: Grant Number 80366), the Welsh Government, the Higher Education Funding Council for Wales, the Welsh European Funding Office, and the European Regional Development Fund Convergence Programme. Jim Freer's time was funded by NERC grant NE/K00882X/1 (SINATRA project), and we would like to thank Gemma Coxon, also at Bristol University, for her time processing the river flow data. T. Coulthard and C. Skinner wish to acknowledge the Environment Agency and the Association of British Ports - Humber Services for the provision of data. Finally, the authors wish to thank

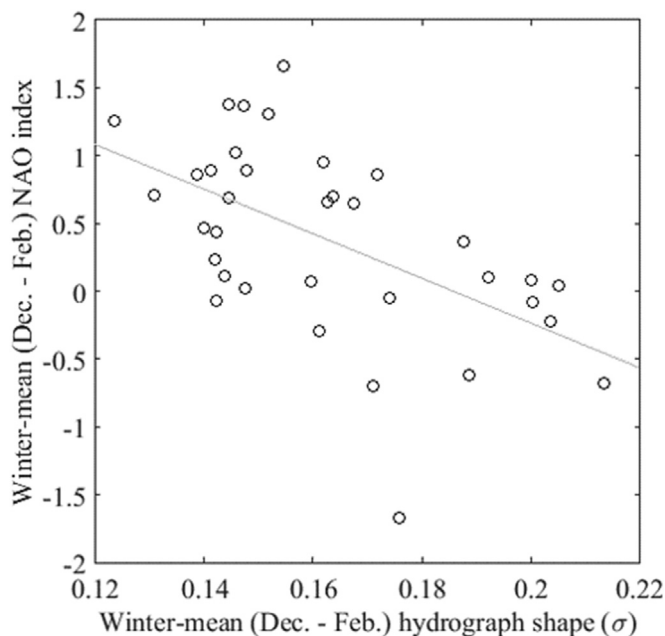


Fig. 8. Correlation between winter-mean hydrograph shape (σ) and winter-mean North Atlantic Oscillation (NAO) index. The linear line of best fit is plotted to show the trend, with a Pearson's Rank correlation of 0.0005, based on 35 samples, and a coefficient of determination $r^2 = 0.25$. See (Neill and Hashemi, 2013) for justification of using winter-mean (Dec-Feb) NAO values.

the reviewers of an earlier draft of the paper for their constructive comments.

Appendix. Modelling description and parameterisation

The Telemac Modelling System (TELEMAC-2D, V7.0; www.opentelemac.org) uses an unstructured-mesh bathymetric grid to drive a hydrostatic ocean model. We applied Telemac to the Conwy and Humber estuaries, UK. The model is based on the depth-averaged shallow water Saint-Venant equations of momentum and continuity, derived from the Navier–Stokes equations (Hervouet, 2007). The classical $k-\epsilon$ turbulence model has been adapted into vertically averaged form to include additional dispersion terms (Rastori and Rodi, 1978); a constant internal friction coefficient of $3 \times 10^{-2} \text{ m}$ was implemented in Nikuradse's law of bottom friction (Hervouet, 2007). Turbulent viscosity has been set constant with the overall viscosity (molecular + turbulent) coefficient equal to 10^{-6} .

For the Conwy, the unstructured mesh, created using Blue-kenue[®], has a resolution of approximately 15 m within the estuary and coarser (50–500 m) offshore. The mesh was mapped onto a bathymetric grid comprising Admiralty data (EDINA, 2008), LIDAR data in intertidal regions (available from Natural Resources Wales), and single-beam echosounder surveys of the sub-tidal estuary channel which was conducted by Bangor University in 2003. More information about the model setup and its validation can be found in Robins et al. (2014). For the Humber, bathymetric data used for a validated model (see Skinner et al., 2015), was provided at 100 m spatial resolution by the University of Hull.

Each model was initially spun-up to create a steady-state salinity balance under minimum river flow conditions and a mean tidal regime (i.e., forced with M_2 and S_2 tidal constituents only at the offshore open boundary). The salinity distribution from these spin-up simulations were used as initial conditions for all subsequent simulations. Comprehensive validation procedures were conducted for each estuary model; see Robins et al. (2014) for the Conwy validation and Skinner et al. (2015) for the Humber validation.

References

- Arnell, N.W., Halliday, S.J., Battarbee, R.W., Skeffington, R.A., Wade, A.J., 2015. The implications of climate change for the water environment in England. *Prog. Phys. Geogr.* 39, 93–120.
- Bell, V.A., Kay, A.L., Cole, S.J., Jones, R.G., Moore, R.J., Reynard, N.S., 2012. How might climate change affect river flows across the Thames Basin? An area-wide analysis using the UKCP09 Regional Climate Model ensemble. *J. Hydrol.* 442–443, 89–104.
- Bevelhimer, M.S., McManamay, R.A., O'Connor, B., 2015. Characterizing sub-daily flow regimes: implications of hydrologic resolution on ecohydrology studies. *River Res. Appl.* 31, 867–879.
- Beven, K.J., Alcock, R.E., 2012. Modelling everything everywhere: a new approach to decision-making for water management under uncertainty. *Freshw. Biol.* 57, 124–132.
- Chan, S.C., Kendon, E.J., Fowler, H.J., Blenkinsop, S., Ferro, C.A.T., Stephenson, D.B., 2013. Does increasing the spatial resolution of a regional climate model improve the simulated daily precipitation? *Clim. Dynam.* 41, 1475–1495.
- Charlton, M.B., Arnell, N.W., 2014. Assessing the impacts of climate change on river flows in England using the UKCP09 climate change projections. *J. Hydrol.* 519, 1723–1738.
- Christierson, B.V., Vidal, J.P., Wade, S.D., 2012. Using UKCP09 probabilistic climate information for UK water resource planning. *J. Hydrol.* 424, 48–67.
- Cloern, J.E., 2001. Our evolving conceptual model of the coastal eutrophication problem. *Mar. Ecol. Prog. Ser.* 210, 223–253.
- Cloke, H.L., Wetterhall, F., He, Y., Freer, J.E., Pappenberger, F., 2013. Modelling climate impact on floods with ensemble climate projections. *Q. J. R. Meteorol. Soc.* 139, 282–297.
- COM, 2014. The First Phase of Implementation of the Marine Strategy Framework Directive (2008/56/EC).
- Coulthard, T.J., Skinner, C.J., 2016. The sensitivity of landscape evolution models to spatial and temporal rainfall resolution. *Earth Surf. Dynam.* 4, 757–771.
- Coulthard, T.J., Ramirez, J., Fowler, H.J., Glenis, V., 2012. Using the UKCP09 probabilistic scenarios to model the amplified impact of climate change on drainage basin sediment yield. *Hydrol. Earth Syst. Sci.* 16, 4401–4416.
- Davidson, N.C., Laffoley, D.A., Doody, J.P., Way, L.S., Gordon, J., Key, R., Pienkowski, M.W., Mitchell, R., Duff, K., 1991. Nature Conservation and Estuaries in Great Britain. Nature Conservancy Council, Peterborough.
- Davies, A.G., Robins, P.E., 2017. Residual flow, bedforms and sediment transport in a tidal channel modelled with variable bed roughness. *Geomorphology* 295, 855–872.
- Elliott, M., Fernandes, T.F., De Jonge, V.N., 1999. The impact of European Directives on estuarine and coastal science and management. *Aquat. Ecol.* 33, 311–321.
- Fowler, H.J., Kilsby, C.G., 2007. Using regional climate model data to simulate historical and future river flows in northwest England. *Climatic Change* 80, 337–367.
- Fowler, H.J., Blenkinsop, S., Tebaldi, C., 2007. Linking climate change modelling to impacts studies: recent advances in downscaling techniques for hydrological modelling. *Int. J. Climatol.* 12, 1547–1578.
- French, J.R., Clifford, N.J., 2000. Hydrodynamic modelling as a basis for explaining estuarine environmental dynamics: some computational and methodological issues. *Hydrol. Process.* 14, 2089–2108.
- Greene, S., Johns, P.J., Bloomfield, J.P., Reaney, S.M., Lawley, R., Elkhatib, Y., Freer, J., Odoni, N., Macleod, C.J.A., Percy, B., 2015. A geospatial framework to support integrated biogeochemical modelling in the United Kingdom. *Environ. Model. Software* 68, 219–232.
- Haktanir, T., Sezen, N., 1990. Suitability of two-parameter gamma and three-parameter beta distributions as synthetic unit hydrographs in Anatolia. *Hydrol. Sci. J.* 35, 167–184.
- Hannaford, J., Harvey, C.L., 2010. UK seasonal river flow variability in near-natural catchments, regional outflows and long hydrometric records. In: Kirby, Celia (Ed.), *Role of Hydrology in Managing Consequences of a Changing Global Environment*. British Hydrological Society Third International Symposium. British Hydrological Society, Newcastle, pp. 96–102.
- Hannaford, J., Marsh, T.J., 2008. High-flow and flood trends in a network of undisturbed catchments in the UK. *Int. J. Climatol.* 28, 1325–1338.
- Howlett, E.R., Bowers, D.G., Malarkey, J., Jago, C.F., 2015. Stratification in the presence of an axial convergent front: causes and implications. *Est. Coast. Shelf Sci.* 161, 1–10.
- Hurrell, J.W., 1995. Decadal trends in the North Atlantic oscillation. *Clim. Change: Eval. Recent Future Clim. Change* 4, 201.
- Jarvie, H.P., Neal, C., Tappin, A.D., Burton, J.D., Harrow, M., Hill, L., Neal, M., 2000. The water quality of the River Trent: from the lower non-tidal reaches to the freshwater tidal zone. *Sci. Total Environ.* 251–252, 335–367.
- Jayawardena, A.W., 2014. *Environmental and Hydrological Systems Modelling*. CRC Press, US, ISBN 978-0-415-46532-8.
- Kay, A.L., Jones, D.A., 2012. Transient changes in flood frequency and timing in Britain under potential projections of climate change. *Int. J. Climatol.* 32, 489–502.
- Kay, A.L., Jones, R.G., Reynard, N.S., 2006. RCM rainfall for UK flood frequency estimation. II. Climate change results. *J. Hydrol.* 318, 163–172.
- Kendon, E.J., Roberts, N.M., Fowler, H.J., Roberts, M.J., Chan, S.C., Senior, C.A., 2014. Heavier summer downpours with climate change revealed by weather forecast resolution model. *Nat. Clim. Change* 4, 570–576.
- Landau, H.J., 1967. Necessary density conditions for sampling and interpolation of certain entire functions. *Acta Math.* 117, 37–52.
- Law, M., Wass, P., Grimshaw, D., 1997. The hydrology of the Humber. *Sci. Total Environ.* 194–195, 119–128.
- Lewis, M.J., Bates, P., Horsburgh, K., Smith, R., 2011. Quantifying uncertainty in future flood risk estimates. *J. Coast. Res.* 27, 870–881.
- Liu, R.M., Chen, Y.X., Sun, C.C., Zhang, P.P., Wang, J.W., Yu, W.W., Shen, Z.Y., 2014. Uncertainty analysis of total phosphorus spatial-temporal variations in the Yangtze River Estuary using different interpolation methods. *Mar. Pollut. Bull.* 86, 68–75.
- Lotze, H.K., Lenihan, H.S., Bourque, B.J., Bradbury, R.H., Cooke, R.G., Kay, M.C., Kidwell, S.M., Kirby, M.X., Peterson, C.H., Jackson, J.B.C., 2006. Depletion, degradation, and recovery potential of estuaries and coastal seas. *Science* 312, 1806–1809.
- Malham, S.K., Rajko-Nenow, P., Howlett, E., Tuson, K.E., Perkins, T.L., Pallett, D.W., Wang, H., Jago, C.F., Jones, D.L., McDonald, J.E., 2014. The interaction of human microbial pathogens, particulate material and nutrients in estuarine environments and their impacts on recreational and shellfish waters. *Environ. Sci. Process. Impacts* 16, 2145–2155.
- McMillan, H., Krueger, T., Freer, J., 2012. Benchmarking observational uncertainties for hydrology: rainfall, river discharge and water quality. *Hydrol. Process.* 26, 4078–4111.
- Mitchell, S.B., West, J.R., Arundale, A.M.W., Guymier, I., Couperthwaite, J.S., 1998. Dynamics of the turbidity maxima in the upper humber estuary system, UK. *Mar. Pollut. Bull.* 37, 190–205.
- Monk, W.A., Wood, P.J., Hannah, D.M., Wilson, D.A., Extence, C.A., Chadd, R.P., 2006. Flow variability and macroinvertebrate community response within riverine systems. *River Res. Appl.* 22, 595–615.
- Monte, L., Hakanson, L., Perianez, R., Laptev, G., Zheleznyak, M., Maderich, V., Angeli, G., Koshebutsky, V., 2006. Experiences from a case study of multi-model application to assess the behaviour of pollutants in the Dnieper-Bug Estuary. *Ecol. Model.* 195, 247–263.
- Naiman, R.J., Latterell, J.J., Pettit, N.E., Olden, J.D., 2008. Flow variability and the biophysical vitality of river systems. *Compt. Rendus Geosci.* 340, 629–643.

- Neill, S.P., Hashemi, M.R., 2013 Jun 1. Wave power variability over the northwest European shelf seas. *Appl. Energy* 106, 31–46.
- OSPAR Commission, 2009. Evaluation of the OSPAR system of ecological quality objectives for the North sea. *Biodivers. Ser.* 102.
- Prudhomme, C., Davies, H., 2009a. Assessing uncertainties in climate change impact analyses on the river flow regimes in the UK. Part 1: baseline climate. *Climatic Change* 93, 177–195.
- Prudhomme, C., Davies, H., 2009b. Assessing uncertainties in climate change impact analyses on the river flow regimes in the UK. Part 2: future climate. *Clim. Change* 93, 197–222.
- Prudhomme, C., Dadson, S., Morris, D., Williamson, J., Goodsell, G., Crooks, S., Boelee, L., Davies, H., Buys, G., Lafon, T., Watts, G., 2012. Future flows Climate: an ensemble of 1-km climate change projections for hydrological application in Great Britain. *Earth Syst. Sci. Data* 4, 143–148.
- Robins, P.E., Lewis, M.J., Simpson, J.H., Howlett, E.R., Malham, S.K., 2014. Future variability of solute transport in a macrotidal estuary. *Estuar. Coast Shelf Sci.* 151, 88–99.
- Robins, P.E., Skov, M.W., Lewis, M.J., Giménez, L., Davies, A.G., Malham, S.K., Neill, S.P., McDonald, J.E., Whitton, T.A., Jackson, S.E., Jago, C.F., 2016. Impact of climate change on UK estuaries: a review of past trends and potential projections. *Estuar. Coast Shelf Sci.* 169, 119–135.
- Rügner, H., Schwientek, M., Egnér, M., Grathwohl, P., 2014. Monitoring of event-based mobilization of hydrophobic pollutants in rivers: calibration of turbidity as a proxy for particle facilitated transport in field and laboratory. *Sci. Total Environ.* 490, 191–198.
- Savenije, H.H.G., 2006. *Salinity and Tides in Alluvial Estuaries*. Elsevier.
- Simpson, J.H., Vennell, R., Souza, A.J., 2001. The salt fluxes in a tidally energetic estuary. *Estuar. Coast Shelf Sci.* 52, 131–142.
- Skinner, C.J., Coulthard, T.J., Parsons, D.R., Ramirez, J.A., Mullen, L., Manson, S., 2015. Simulating tidal and storm surge hydraulics with a simple 2D inertia based model, in the Humber Estuary, UK. *Estuar. Coast Shelf Sci.* 155, 126–136.
- Smith, A., Freer, J., Bates, P., Sampson, C., 2014a. Comparing ensemble projections of flooding against flood estimation by continuous simulation. *J. Hydrol.* 511, 205–219.
- Smith, A., Bates, P., Freer, J., Wetterhall, F., 2014b. Investigating the application of climate models in flood projection across the UK. *Hydrol. Process.* 28, 2810–2823.
- Statham, P.J., 2012. Nutrients in estuaries – an overview and the potential impacts of climate change. *Sci. Total Environ.* 434, 213–227.
- Svensson, C., Hannaford, J., Kundzewicz, Z.W., Marsh, T.J., 2006. Trends in river floods: why is there no clear signal in observations? *IAHS Publ. Proc. Rep.* 305, 1–8.
- Tang, R., Clark, J.M., Bond, T., Graham, N., Hughes, D., Freeman, C., 2013. Assessment of potential climate change impacts on peatland dissolved organic carbon release and drinking water treatment from laboratory experiments. *Environ. Pollut.* 173, 270–277.
- Townend, I., Whitehead, P., 2003. A preliminary net sediment budget for the Humber Estuary. *Sci. Total Environ.* 314–316, 755–767.
- Trigo, R.M., Pozo-Vázquez, D., Osborn, T.J., Castro-Díez, Y., Gámiz-Fortis, S., Esteban-Parra, M.J., 2004. North Atlantic Oscillation influence on precipitation, river flow and water resources in the Iberian Peninsula. *Int. J. Climatol.* 24, 925–944.
- Uncles, R.J., Easton, A.E., Griffiths, M.L., Harris, C., Howland, R.J.M., King, R.S., Morris, A.W., Plummer, D.H., 1999. Seasonality of the turbidity maximum in the humber-ouse estuary, UK. *Mar. Pollut. Bull.* 37, 206–215.
- Uncles, R.J., Stephens, J.A., Law, D.J., 2006. Turbidity maximum in the macrotidal, highly turbid Humber Estuary, UK: flocs, fluid mud, stationary suspensions and tidal bores. *Estuar. Coast Shelf Sci.* 67, 30–52.
- Wade, A.J., Neal, C., Whitehead, P.G., Flynn, N.J., 2005. Modelling nitrogen fluxes from the land to the coastal zone in European systems: a perspective from the INCA project. *J. Hydrol.* 304, 413–429.
- Wilby, R.L., Beven, K.J., Reynard, N.S., 2008. Climate change and fluvial flood risk in the UK: more of the same? *Hydrol. Process.* 22, 2511–2523.
- Wilkinson, J., Kay, D., Wyer, M., Jenkins, A., 2006. Processes driving the episodic flux of faecal indicator organisms in streams impacting on recreational and shellfish harvesting waters. *Water Res.* 40, 153–161.

Appendix references

- EDINA Marine Digimap Service, 2008. *Hydrospatial Bathymetry, Scale 1: 45,000, Tiles: NW25000040-NW25000080, NW25200040-NW25200080, NW25400040-NW25400080*. SeaZone Solutions Ltd, UK. Updated April.
- Hervouet, J.M., 2007. *Hydrodynamics of Free Surface Flows*, first ed. John Wiley and Sons, Press.
- Rastori, A.-K., Rodi, W., 1978. Predictions of heat and mass transfer in open channels. *J. Hydraul. Div.* 104, 397–420.
- Skinner, C.J., Coulthard, T.J., Parsons, D.R., Ramirez, J.A., Mullen, L., Manson, S., 2015. Simulating tidal and storm surge hydraulics with a simple 2D inertia based model, in the Humber Estuary, UK. *Estuar. Coast Shelf Sci.* 155, 126–136.
- Robins, P.E., Lewis, M.J., Simpson, J.H., Howlett, E.R., Malham, S.K., 2014. Future variability of solute transport in a macrotidal estuary. *Estuar. Coast Shelf Sci.* 151, 88–99.